






# Gutter Characteristics and Stent Compression of Self-Expanding vs Balloon-Expandable Chimney Grafts in Juxtarenal Aneurysm Models

Jorn P. Meekel, MD<sup>1,2,3\*</sup> , Theodorus G. van Schaik, MD<sup>1,2,3\*</sup> ,  
Rutger J. Lely, MD<sup>4</sup>, Gerie Groot, MD<sup>4</sup>, Bram B. van der Meijs, MD<sup>4</sup>,  
Willem Wisselink, MD, PhD<sup>1</sup>, Jan D. Blankensteijn, MD, PhD<sup>1</sup>,  
and Kak K. Yeung, MD, PhD<sup>1,2</sup> 

## Abstract

**Purpose:** To assess in silicone juxtarenal aneurysm models the gutter characteristics and compression of different types of chimney graft (CG) configurations. **Materials and Methods:** Fifty-seven combinations of Excluder C3 or Conformable Excluder stent-grafts (23, 26, and 28.5 mm) were deployed in 2 silicone juxtarenal aneurysm models with 3 types of CGs: Viabahn self-expanding (VSE; 6 and 13 mm) or Viabahn balloon-expandable (VBX; 6, 10, and 12 mm) stent-grafts and Advanta V12 balloon-expandable stent-grafts (ABX; 6 and 12 mm). Setups were divided into 4 groups on the basis of increasing CG and main graft (MG) diameters. Two independent observers assessed gutter size and type as well as CG compression on computed tomography scans using postprocessing software. **Results:** In the smaller diameter combinations (6-mm CG and 23-, 26-, and 28.5-mm MGs), both VSE ( $p=0.006$  to  $0.050$ ) and ABX ( $p=0.045$  to  $0.050$ ) showed lower gutter areas and volumes compared with VBX. In turn, the VBX showed a nonsignificant tendency to decreased compression, especially compared to ABX. Use of the Excluder C3 showed a 6-fold increase in type A1 gutters (related to type Ia endoleak) as compared to the Conformable Excluder ( $p=0.018$ ). Balloon-expandable stent-grafts (both ABX and VBX) showed a 3-fold increase in type A1 gutters in comparison with self-expanding stent-grafts ( $p=0.008$ ). **Conclusion:** The current study suggests that use of the Conformable Excluder in combination with VSE chimney grafts is superior to the other tested CG/MG combinations in terms of gutter size, gutter type, and CG compression.

## Keywords

balloon-expandable stent-graft, chimney graft, compression, endoleak, endovascular repair, gutter, gutter type, in vitro model, juxtarenal aneurysm model, self-expanding stent-graft

## Introduction

Complex fenestrated/branched endovascular aneurysm repair (f/bEVAR) with customized devices is not applicable in the emergency or urgent setting due to the minimum 4-week manufacturing time.<sup>1,2</sup> Although off-the-shelf fenestrated and branched solutions exist, the majority of patients with juxtarenal, pararenal, and suprarenal aortic aneurysms do not meet the anatomical criteria for EVAR with these devices.<sup>3</sup> Endovascular repair of complex aneurysms with off-the-shelf chimney EVAR (chEVAR) configurations is an alternative. In this technique, parallel stent-grafts are deployed adjacent to the main graft (MG) to maintain perfusion into the renovisceral branches after aneurysm exclusion.<sup>4-6</sup> This technique is used not only for bailout procedures but also for

<sup>1</sup>Department of Vascular Surgery, Amsterdam University Medical Centers, VU Medical Center, Amsterdam, the Netherlands

<sup>2</sup>Department of Physiology, Amsterdam University Medical Centers, VU Medical Center, Amsterdam Cardiovascular Sciences, Amsterdam, the Netherlands

<sup>3</sup>Department of Surgery, Zaans Medisch Centrum, Zaandam, the Netherlands

<sup>4</sup>Department of Interventional Radiology, Amsterdam Medical Centers, VU Medical Center, Amsterdam, the Netherlands

\*Jorn P. Meekel and Theodorus G. van Schaik contributed equally to this work and have shared first authorship.

### Corresponding Author:

Kak K. Yeung, Departments of Surgery and Physiology, Amsterdam University Medical Centers, Amsterdam Cardiovascular Sciences, De Boelelaan 1118, 1081 HV, Amsterdam, the Netherlands.  
Email: k.yeung@amsterdamumc.nl

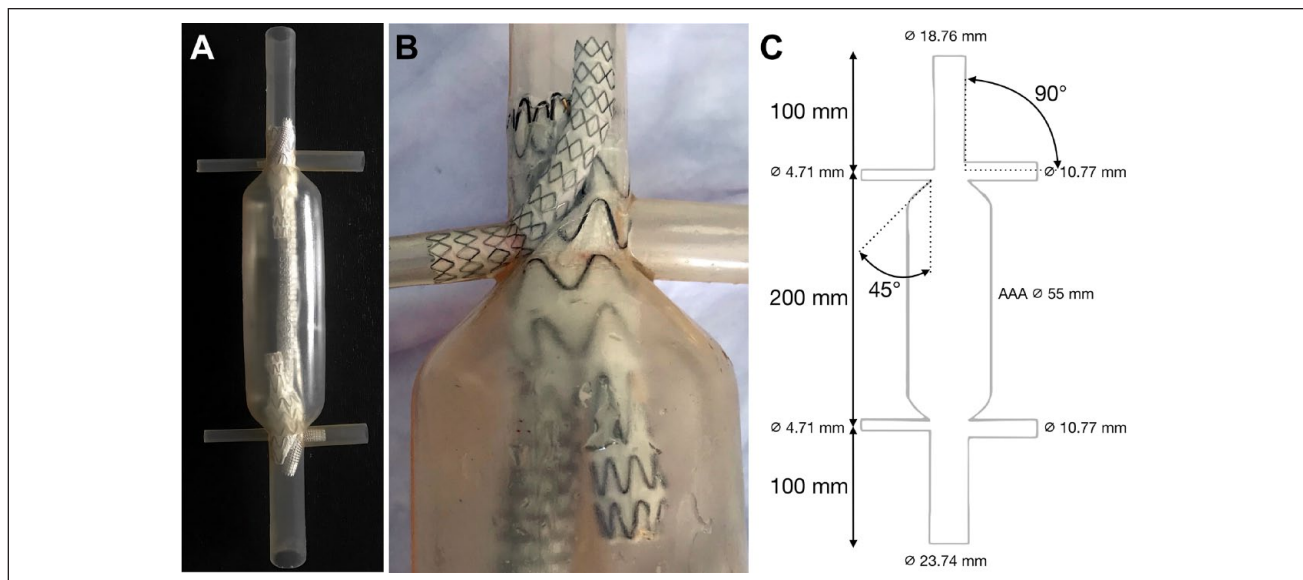


**Figure 1.** (A) Silicone aortic aneurysm model with main graft and chimney graft deployed for analysis. (B) Close-up of in vitro chimney configuration of a Viabahn balloon-expandable stent-graft in combination with a Conformable Excluder. The different diameters of the renal arteries can be seen. (C) Schematic overview of silicone aneurysm model including inner diameters of the aorta and branches and lengths and angles of the branches.

elective cases in daily practice all over the world.<sup>7-9</sup> The advantages include availability in emergent situations and lower costs than custom-made f/bEVAR devices. In many countries, custom-made devices are not available and chEVAR may be the only viable endovascular therapy.

Mid- to long-term outcomes of chEVAR are promising,<sup>8-10</sup> but reintervention remains a topic of discussion. Recent systematic reviews and meta-analyses comparing f/bEVAR and chEVAR conclude that both surgical techniques might be beneficial in patients with various baseline characteristics and anatomies. Therefore, both techniques should remain part of the physicians' armamentarium for the treatment of complex aortic aneurysms.<sup>11,12</sup>

One specific issue of the chimney technique is the occurrence of so-called gutters, formed by an unfilled space between the main graft, chimney, and aortic wall due to imperfect apposition.<sup>13</sup> These gutters are associated with the development of type Ia endoleaks, potentially leading to fatal aneurysm rupture.<sup>7</sup> As these stent-grafts are not designed to be deployed next to each other, graft compression or kinking can also influence the patency of the grafts. The frequency of early type I endoleaks is relatively low (6.0%–7.6%) and the need for treatment rare.<sup>11,12,14,15</sup> Small gutters are expected to thrombose spontaneously.<sup>16</sup> With the availability of new stents and stent-graft designs for aortic aneurysm repair, new chEVAR configurations can be tailored to the individual patient.

The aim of the current in vitro study was to assess cross-sectional areas, volumes, type of gutters, and compression in different chEVAR configurations using newer chimney grafts (CGs).

## Materials and Methods

### Experimental Setup

Juxtarenal aortic aneurysms were simulated in 2 identical double-branched silicone models fabricated for previous chimney experiments. The models had a wall compliance mimicking the human aorta.<sup>17</sup> Each silicone model (Figure 1) had 2 different aortic diameters (18.76 and 23.74 mm), and both aortic diameters were combined with 2 different renal branch diameters (4.71 and 10.77 mm) to deploy different MG and CG configurations. During deployment of stent-grafts and computed tomography (CT) scanning, the silicone models were completely submerged in a gelatin-water solution (Sigma Chemical Corporation, St Louis, MO, USA) with the viscosity of blood.<sup>18,19</sup> The solution was maintained at a constant 37 °C using a Julabo heating circulator (Julabo USA Inc., Allentown, PA, USA).

### Stent-Grafts

In the current study, results of previously published chEVAR experiments from our research group<sup>17,21</sup> were compared to results of newly performed experiments with new MGs and CGs. In the new experiments, the 23- and 28.5-mm Gore Excluder C3 (GE) and 23-, 26-, and 28.5-mm Gore Conformable Excluder (GCE) stent-grafts (Gore Medical, Flagstaff, AZ, USA) were tested in combination with 3 different types of CGs: the 6- and 13-mm Viabahn self-expanding (VSE) stent-graft (Gore Medical), the 6- and

**Table 1.** Total TP2 and TP3 Gutter Areas, Gutter Volume, and CG Compression.

Setup	MG Type and Diameter, mm	CG Type and Diameter, mm	N <sup>a</sup>	Total Gutter Area TP2 / TP3, <sup>b</sup> mm <sup>2</sup>	Gutter Volume/cm Sealing Zone, <sup>b</sup> cm <sup>3</sup>	CG Compression, <sup>b</sup> %	Gutter Types Other Than A3, <sup>b,c</sup> % (Type)
1 <sup>d</sup>	GE 23	VSE 6	2	21.7 / 19.0	0.14	31.0	—
2 <sup>d</sup>	GE 28.5	VSE 6	2	27.6 / 25.3	0.12	30.6	—
3 <sup>d</sup>	GE 28.5	VSE 13	2	29.4 / 31.0	0.23	18.9	75 (A1)
4 <sup>d</sup>	GE 23	ABX 6	4	30.8 / 25.6	0.17	44.0	50 (A1)
5 <sup>d</sup>	GE 28.5	ABX 6	4	54.1 / 38.0	0.16	37.7	50 (A1)
6 <sup>d</sup>	GE 28.5	ABX 12	2	42.1 / 42.1	0.27	28.7	25 (A1), 25 (C)
7	GE 23	VBX 6	1	29.1 / 19.0	0.22	15.7	50 (A1)
8	GE 28.5	VBX 6	1	48.7 / 53.4	0.59	21.8	100 (A1)
9	GE 28.5	VBX 10	1	38.6 / 41.1	0.50	6.6	100 (A1)
10 <sup>e</sup>	GE 28.5	VBX 12	2	53.7 / 47.4	0.45	0	75 (A1)
11	GCE 23	VSE 6	4	27.6 / 33.0	0.18	33.6	—
12	GCE 26	VSE 6	4	23.7 / 28.3	0.20	35.9	—
13	GCE 28.5	VSE 6	4	22.7 / 35.0	0.26	31.2	—
14 <sup>e</sup>	GCE 28.5	VSE 10	3	64.0 / 44.2	0.34	13.2	17 (A1)
15	GCE 23	VBX 6	4	35.7 / 38.3	0.26	35.1	—
16	GCE 26	VBX 6	4	34.2 / 35.5	0.24	25.3	—
17	GCE 28.5	VBX 6	4	57.4 / 54.4	0.40	31.2	25 (A1)
18 <sup>f</sup>	GCE 28.5	VBX 10	3	84.4 / 58.2	0.41	11.2	17 (A1)
19 <sup>g</sup>	GCE 28.5	VBX 12	3	59.9 / 38.6	0.24	8.0	17 (A1)

Abbreviations: ABX, Advanta balloon-expandable; CG, chimney graft; GCE, Gore Conformable Excluder; GE, Gore Excluder; MG, main graft; TP, table point; VBX, Viabahn balloon-expandable; VSE, Viabahn self-expanding.

<sup>a</sup>Number of repeated experiments.

<sup>b</sup>Median values.

<sup>c</sup>Gutters originating at the proximal start of the main graft fabric can be subdivided into type A1 if continuing into the aneurysm sac, type A2 if continuing into the side branch vessel, or type A3 if terminating proximally to the aneurysm sac and side branch vessel. All gutters were type A3 unless stated otherwise.<sup>16</sup>

<sup>d</sup>Previously published data in part (volumes were additionally measured).<sup>12,15</sup>

<sup>e</sup>In 1 of 2 setups, the CG was inflated from 10 to 12 mm.

<sup>f</sup>One setup was excluded due to deployment complications.

<sup>g</sup>In all setups the CGs were inflated from 10 to 12 mm.

12-mm Advanta V12 balloon-expandable (ABX) stent-graft (Getinge, Gothenburg, Sweden), and the more recently released 6- and 10-mm Viabahn balloon-expandable (VBX) stent-graft (Gore Medical). Furthermore, the 10-mm VBX was additionally inflated to 12 mm. In total, 57 MG and CG combinations (Table 1) were deployed and analyzed. In all the different setups, new main grafts were used, except for the setups in which the VBX was reinflated from 10 to 12 mm. A configuration of a small MG with large CGs was not tested since this configuration has been shown to seriously compress the MG.<sup>17</sup>

All CGs were positioned through the suprarenal aorta over Rosen guidewires (Cook Medical, Bloomington, IN, USA), and the MGs were positioned through the infrarenal aorta. The free flare zone of the CG was 5 mm proximal to the MG, and positions were checked using a ruler. CGs were balloon molded using a balloon inflator; MGs were deployed using a compliant Reliant balloon (Medtronic, Minneapolis, MN, USA). The aim was to deploy MGs and CGs simultaneously; if this was not the case, the MGs and CGs were balloon molded simultaneously for 30 seconds.

Main graft oversizing was 23%, 39%, and 20% for the 23-, 26-, and 28.5-mm MGs, respectively.

### CT Scanning and Measurements

Experimental setups were scanned using a 64-slice CT scanner (Philips Medical Systems, Eindhoven, the Netherlands) with a resolution of 512×512 pixels and a slice thickness of 600 μm. Osirix postprocessing software (Pixmeo, Geneva, Switzerland) was used for geometrical measurements. Four table positions (TPs) were defined: TP1, start of the CG; TP2, start of the MG and sealing zone; TP3, end of the sealing zone; and TP4, CG fully positioned in the branch (Figure 2).

Gutter cross-sectional area (CSAs) and volume measurements were performed using the predefined TPs. Both ventral and dorsal gutter CSAs were manually and consecutively measured from TP2 distally up to TP4. CSAs between TP1 and TP4 were used to analyze the type of gutter. CSAs at TP2 and TP3 were analyzed as individual outcomes, and the consecutive results from the CSAs between TP2 to TP3 were

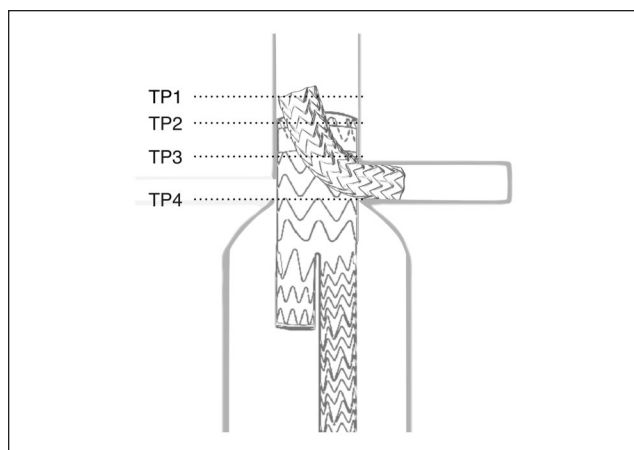


**Figure 2.** Schematic overview of table points (TP) used for gutter analysis. TP1 represents the start of the chimney graft (CG); TP2, the start of the main graft and sealing zone; TP3, the end of the sealing zone; and TP4, the CG fully positioned in the branch.

used to compute 3-dimensional (3D) gutter volumes. Gutter volumes were corrected for seal zone length variations and are presented as gutter volume per centimeter seal zone.

CG lumen area just proximal to TP1 and a central lumen line through the CG were used to calculate the percentage of CG compression based on the maximal (proximal to TP1) and minimal CG lumen areas, which were measured perpendicular to the stent-graft's central lumen line. All gutters were classified as A1–3, B1 or 2, or C (Figure 3) according to the system reported by Overeem et al.<sup>21</sup> Gutter types A1, A2, and A3 originate at the proximal start of the MG fabric and, respectively, continue into the aneurysm sac, side branch vessel, or terminate proximal to the aneurysm sac or CG. Gutter types B1 and B2 are not found in the proximal part of the MG; B1 connects the stented renovisceral artery with the aneurysm sac and B2 is found circumferential to the CG only. Gutter type C is an enclosed volume without any connection to the proximal or distal CG end or continuation into the aneurysm sac. Gutter type A1 is mostly related to antegrade type Ia endoleak and gutter type B1 is related to retrograde type Ib endoleak, both with persistent blood flow into the aneurysm. Therefore, these situations might require reintervention.

To analyze comparable anatomical situations, 4 combinations (Figure 4) were compiled based on lumen and CG diameters from small CGs and small MGs to large CGs and large MGs. Combination i was a MG diameter of 23 or 26 mm (in the 18.76-mm aortic lumen) combined with a CG diameter of 6 mm (VSE, ABX, and VBX); combination iii was a MG diameter of 28.5 mm (in the 23.74-mm aortic lumen) combined with a CG diameter of 6 mm (VSE, ABX, and VBX); combination iii was a MG diameter of 28.5 mm (in the 23.74-mm aortic lumen) combined with a CG diameter of 10 mm (VSE and VBX); and combination iv was a MG diameter of 28.5 mm (in the 23.74-mm aortic lumen)

combined with a CG diameter of 12 or 13 mm (13-mm VSE, 12-mm ABX, and 10-mm VBX inflated to 12 mm within the instructions for use). The results of the different CGs were compared within each combination. Furthermore, the combined results of the MGs and CGs between the different combinations were assessed to explore differences between anatomical variations.

### Statistical Analysis

The results are presented as the median. Gutter types are presented as the number (percentage). Differences between groups were analyzed with the Mann-Whitney *U* test. TP area compression and measurements were performed in duplicate by 2 independent analysts and averaged. An interobserver reproducibility analysis was performed based on all MG and CG combinations. The intraclass correlation coefficient (ICC) was used to analyze gutter area and compression measurements (the gutter areas were used to compute 3D gutter volume); indexes are given with the 95% confidence interval (CI). According to Koo and Li,<sup>22</sup> an ICC <0.50 indicated poor agreement, an ICC between 0.50 and 0.75 indicated fair agreement, an ICC between 0.75 and 0.90 indicated good agreement, and an ICC >0.90 indicated excellent agreement. The threshold of statistical significance was  $p < 0.05$ . Statistical analyses were performed using SPSS software (version 25.0; IBM Corporation, Armonk, NY, USA).

## Results

### Deployment

The MG and CG configurations were successfully deployed in 54 of 57 setups (95%). The GE was deployed simultaneously with all types of CGs, while the GCE was deployed simultaneously with the ABX and the VBX. The GCE and the VSE CG, however, could not be deployed simultaneously since the preloaded deployment wires of the VSE could accidentally snag the barbs of the GCE's sealing cuff, perhaps blocking the VSE from unfolding. These barbs are more prominent in the GCE than in the conventional GE.

Two types of technical failures occurred in 3 setups. A 10- $\times$ 59-mm VBX in combination with a 28.5-mm GCE was positioned proximally in the branch; when the VBX was inflated from 10 to 12 mm, it migrated completely out of the branch because the stent length in the branch was too short. A 10- $\times$ 50-mm VSE in combination with a 28.5-mm GCE also was not inserted deeply enough in the branch and lacked a flare zone. These 3 setups were excluded from further analysis.

### Gutter Areas

Since there was no difference between the 2 Excluder models ( $p = 0.251$  for TP2 and  $p = 0.159$  for TP3), the results of the MGs were combined. Gutter areas of TP2 and TP3 are

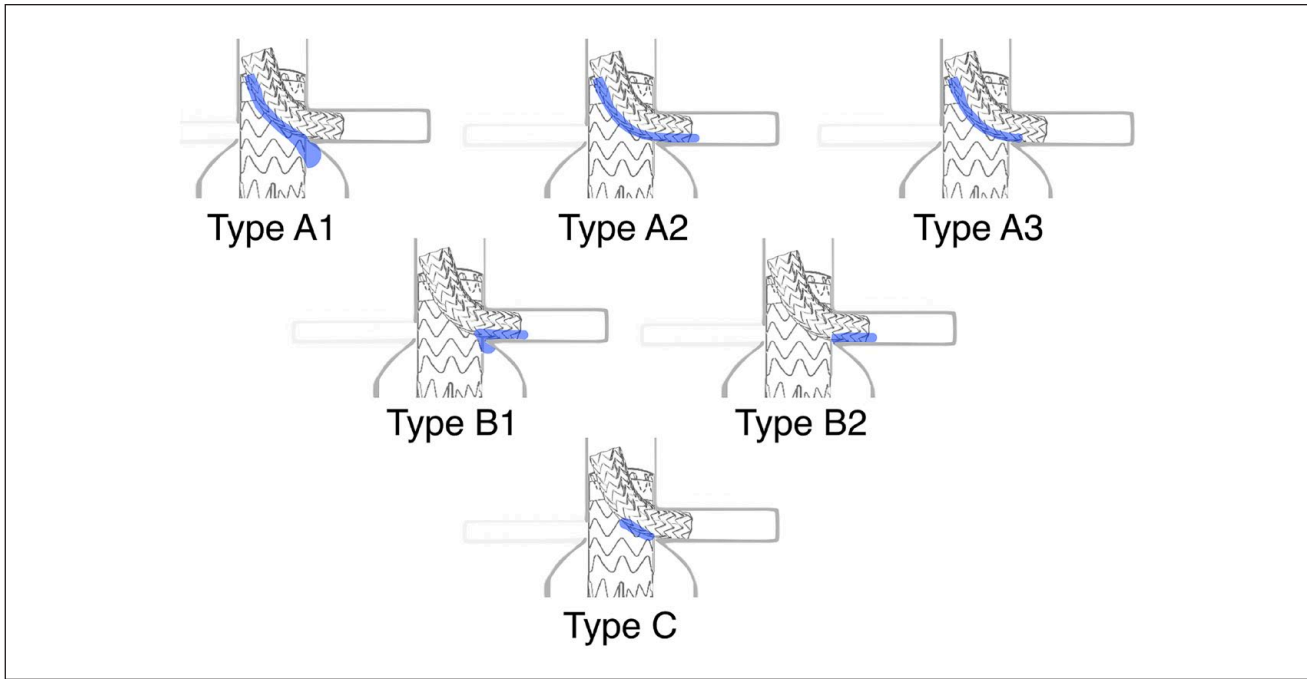


**Figure 3.** Gutter types. Type A1 originates at the start of the main graft fabric and continues into the aneurysm sac, type A2 originates at the start of the fabric and continues into the side branch vessel, and type A3 originates at the start of the fabric and terminates proximally to both the sac and chimney graft (CG). Type B1 connects the renovisceral artery to the aneurysm sac, and type B2 is found only between the CG and the renovisceral artery wall. Type C is found between the CG and main graft, without any connection to a renovisceral artery or the aneurysm sac.

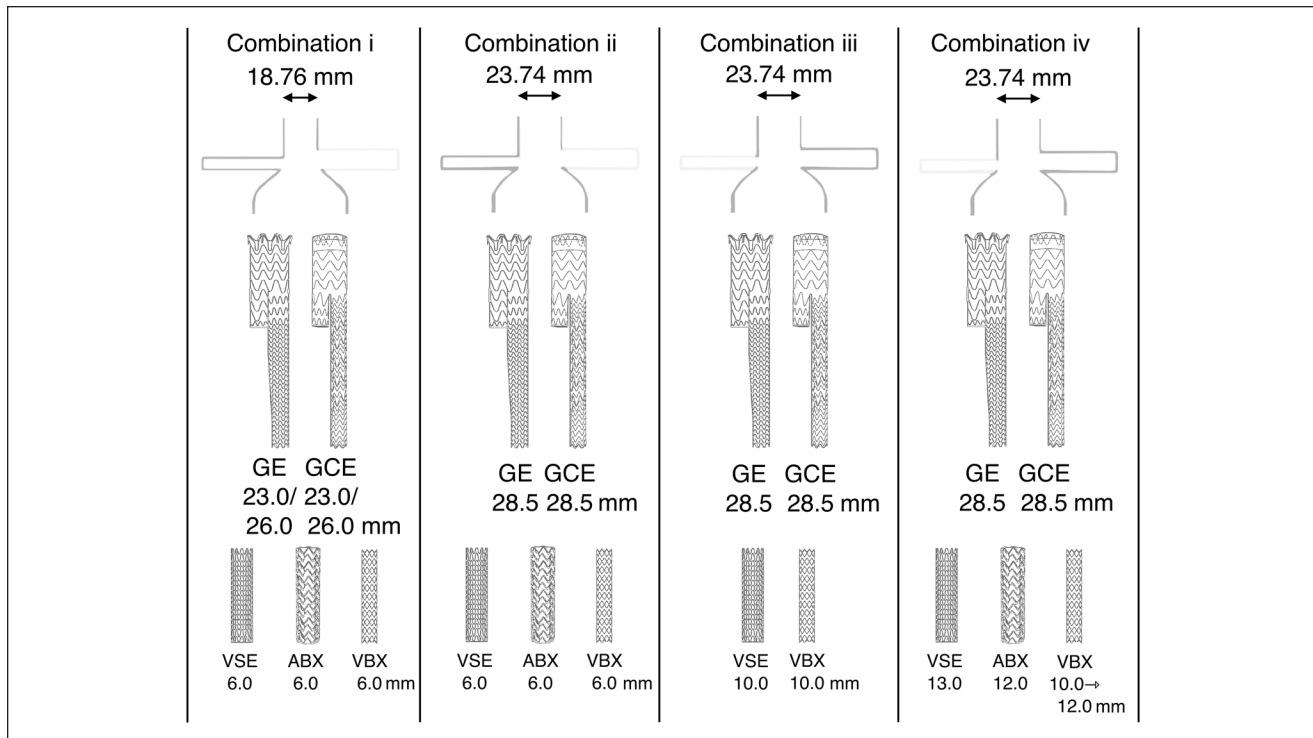


**Figure 4.** An overview of the different combinations of aortic neck diameters, main grafts, and chimney grafts that were grouped for further analysis. All diameters are in millimeters. ABX, Advanta balloon-expandable; GE, Gore Excluder; GCE, Gore Conformable Excluder; VBX, Viabahn balloon-expandable; VSE, Viabahn self-expanding.

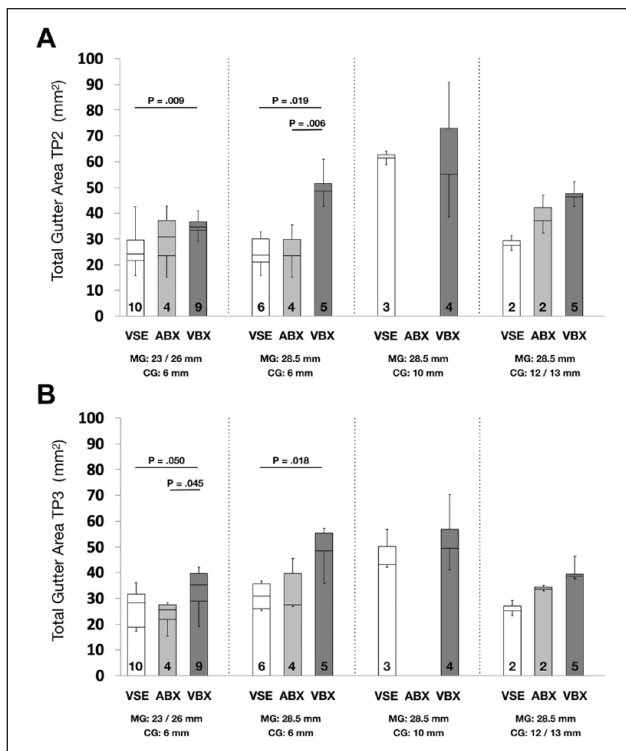


**Figure 5.** Median total gutter areas compared between and within groups at (A) TP2 and (B) TP3. Numbers of repeated measurements are presented at the bottom of the bars;  $p < 0.05$  indicates a statistically significant difference. ABX, Advanta balloon-expandable; CG, chimney graft; MG, main graft; TP, table point; VBX, Viabahn balloon-expandable; VSE, Viabahn self-expanding.

presented in Table 1. Box plots of gutter area results are shown in Figure 5.

At TP2 (top of the sealing zone), VSE CGs had overall the lowest gutter areas when compared to VBX ( $p=0.009$  for combination i and  $p=0.019$  for combination ii). ABX showed lower gutter areas compared to VBX in combination ii ( $p=0.006$ ). At TP3 (bottom of the sealing zone), VSE CGs had overall the lowest gutter areas when compared to VBX ( $p=0.050$  for combination i and  $p=0.018$  for combination ii). ABX showed lower gutter areas compared to VBX in combination i ( $p=0.045$ ).

### Gutter Volumes and CG Compression

The 3D gutter volumes (Table 1) of the VSE CGs were lowest compared with VBX ( $p=0.018$  for combination i and  $p=0.006$  for combination ii). ABX showed lower 3D gutter volumes compared to VBX in combination ii ( $p=0.050$ ). A nonsignificant trend of lower compression was observed in the VBX, mostly compared to the ABX. Box plots of gutter volumes per cm sealing zone and CG compression are shown in Figure 6A and B, respectively.

### Comparison Between Groups

An assessment between the different MG and CG combinations was performed to evaluate the outcomes in different anatomical variations, which are bundled in the predefined combinations i to iv (as shown in Figure 4) and consecutively ordered from small CG / small MG (combination i) to large CG / large MG (combination iv). In general, smaller CG/MG combinations showed smaller gutters and higher CG compression; however, results of combination iv (large CG and large MG) showed an opposite tendency.

At TP2, lower gutter areas were observed for combinations i vs iii ( $30.9$  vs  $64.0$   $\text{mm}^2$ ,  $p < 0.001$ ), combinations i vs iv ( $30.9$  vs  $46.4$   $\text{mm}^2$ ,  $p=0.005$ ), and combinations ii vs iii ( $32.7$  vs  $64.0$   $\text{mm}^2$ ,  $p=0.022$ ). Conversely, higher gutter areas were observed in combinations iii vs iv ( $64.0$  vs  $46.4$   $\text{mm}^2$ ,  $p=0.039$ ).

At TP3, lower gutter areas were observed for combinations i vs ii ( $29.0$  vs  $36.2$   $\text{mm}^2$ ,  $p=0.012$ ), combinations i vs iii ( $29.0$  vs  $52.2$   $\text{mm}^2$ ,  $p < 0.001$ ), and combinations i vs iv ( $29.0$  vs  $37.6$   $\text{mm}^2$ ,  $p=0.020$ ). Again, higher gutter areas were seen in combinations iii vs iv ( $52.2$  vs  $36.7$   $\text{mm}^2$ ,  $p=0.010$ ).

Overall 3D gutter volumes per cm sealing zone were lower in combinations i vs iii ( $0.22$  vs  $0.41$   $\text{cm}^3$ ,  $p=0.001$ ). Furthermore, mean CG compression was higher in combinations i vs iii ( $35.0$  vs  $11.2$   $\text{mm}^2$ ,  $p < 0.001$ ), combinations i vs iv ( $35.0$  vs  $8.5$   $\text{mm}^2$ ,  $p < 0.001$ ), combinations ii vs iii ( $31.7$  vs  $8.5$   $\text{mm}^2$ ,  $p < 0.001$ ), and combinations ii vs iv ( $31.7$  vs  $8.5$   $\text{mm}^2$ ,  $p < 0.001$ ).

### Gutter Types

Gutter type classification found 25 (23%) type A1 gutters (with continuation into the aneurysm sac), no type A2 gutters, and 82 (76%) type A3 gutters. No type B1 or B2 gutters were observed, and 1 (1%) type C gutter was encountered. In setups using the conventional GE stent-graft, 20 (48%) type A1 gutters were found, while in setups using the GCE stent-graft, 5 (8%) type A1 gutters were found ( $p=0.018$ ). Setups involving self-expanding stent-grafts showed 4 (10%) type A1 gutters, while setups involving balloon-expandable stent-grafts (both ABX and VBX) showed 21 (32%) type A1 gutters ( $p=0.008$ ). Gutters different than type A3 gutters are presented in Table 1.

### Interrater Reliability

An excellent degree of reliability was found between measurements for TP2 and TP3 areas and CG compression. The average ICC for TP2 was 0.97 (95% CI 0.95 to 0.98,  $p < 0.001$ ). The average ICC for TP3 was 0.98 (95% CI 0.96 to 0.99,  $p < 0.001$ ). The average ICC for CG compression was 0.90 (95% CI 0.80 to 0.95,  $p < 0.001$ ).

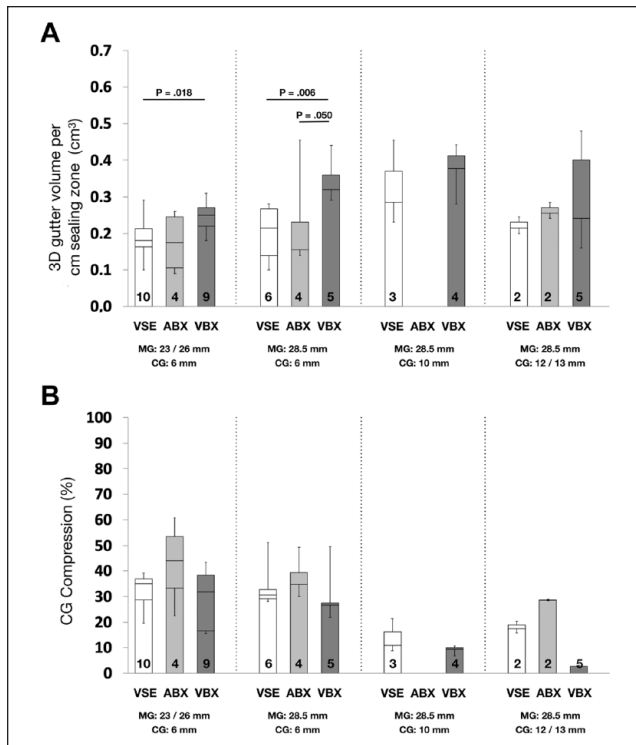


**Figure 6.** (A) Median 3-dimensional gutter volumes per cm sealing zone and (B) median chimney graft compression percentages compared between and within groups. Numbers of repeated measurements are presented at the bottom of the bars;  $p < 0.05$  indicates a statistically significant difference. ABX, Advanta balloon-expandable; CG, chimney graft; MG, main graft; VBX, Viabahn balloon-expandable; VSE, Viabahn self-expanding.

## Discussion

The chEVAR technique has been shown to be a safe, effective, and durable alternative for the treatment of complex aortic aneurysms,<sup>7,14</sup> with low early mortality, few complications, and high long-term patency. Endoleaks can mostly be sealed endovascularly. Continued use in elective, urgent, and emergency settings is therefore advised if local hospital capabilities, timing, specific patient characteristics, and anatomical situations make fEVAR less desirable.<sup>7-9,14</sup> Furthermore, chEVAR could be advised in the post-EVAR setting to treat type Ia endoleaks.<sup>23</sup> Newer alternatives, including physician-modified endovascular grafts and in situ fenestration, seem promising; however, supportive literature is still scarce.<sup>24-27</sup> Therefore, these treatment alternatives are typically considered only when other treatment options are lacking.

Both self-expanding and balloon-expandable CGs are available for use in chEVAR configurations. Recently, new endografts, such as the VBE have become available on the market and are used in chimney configurations.<sup>28</sup> The endografts used in the chimney technique are not designed or typically indicated to be deployed alongside each other.

Therefore, new experiments were considered necessary to test both the self-expanding and balloon-expandable Viabahn models.<sup>29</sup>

Analysis of various CG/MG combinations showed that in general gutter areas at TP2 and TP3 were lower in VSE and ABX compared with VBX. The 3D gutter volumes were lower in VSE and ABX compared to VBX in the 6-mm CGs. No intragroup differences were found for compression between different CGs. Results of the gutter classification as described by Overeem et al<sup>21</sup> imply that self-expanding stent-grafts, compared with their balloon-expandable counterparts, lead to type A1 gutters less frequently. These lower gutter areas and 3D volumes in VSE and ABX seem to come at the expense of a nonsignificant but repeatedly observed higher CG compression, especially when comparing ABX to VBX.

Previously, Boersen et al<sup>30</sup> showed less compression in the balloon-expandable Advanta V12 compared to the self-expanding Viabahn based on the ratio of the major to minor diameters of the graft lumens. However, Mestres et al<sup>29</sup> showed that this ratio of deformation per axial slice was not of clinical importance. Rather, the ratio of the maximum and minimum CSAs between these 2 slices circumferential to the CG's central lumen line was of clinical importance. This is illustrated by the fact that the flow rate is determined mainly by the CSA and only partially by the shape (or diameters) of the artery or CG, as explained by the Bernoulli and Hagen-Poiseuille equations.<sup>31,32</sup> Nonetheless, more accurate measurements can be derived from computational fluid dynamics or 4D flow magnetic resonance imaging data, taking pulsatility of blood flow into consideration.

In the setups in which 6-mm CGs were used, lower gutter areas at TP2 and TP3 were found compared to the larger CGs (10 and 12 or 13 mm). Interestingly, the 10-mm setups showed higher gutter areas at TP2 and TP3 compared to the 12- or 13-mm CGs. Retrospectively reviewing the measurements showed that the MG and CG were better aligned in the 12- and 13-mm CG setups compared to the 10-mm setup. While the 6-mm CG resulted in small gutters as a consequence of the smaller diameter, the smaller gutters in the 12- and 13-mm CG setups might be explained as a consequence of the elliptical shape, leading to better alignment and fewer gutters. CG compression, however, was higher in all 6-mm CGs compared with 10-, 12- and 13-mm CGs. Outcomes of the setups in which the 10.77-mm renal artery was studied might also aid physicians in their decision for chEVAR involving superior mesenteric arteries or celiac trunks, since these generally have larger diameters than renal arteries.

## Limitations

A limitation of the current study was the use of only one type of silicone aortic aneurysm model. Although 2

different suprarenal aortic diameters were combined with 2 different branch diameters, this does not represent the broad range of anatomical variations seen in the aorta, renovisceral branches, and aneurysms, which are of importance for the clinical outcome.<sup>33</sup> Also, the models do not have an infrarenal neck, while the only currently approved chEVAR configuration requires an infrarenal neck length of at least 2 mm. This might lead to a worse outcome in sealing and may thereby affect the percentage of type A1 gutters. General conclusions, however, can be drawn from these combinations considering small and large MGs and CGs.

Also, no fixation of the renal arteries was performed, which might lead to less compression or kinking of the stents at the origins of the renal arteries. Moreover, the stent-grafts were fixed only proximally, so the lack of distal limbs could allow the device to shift. Another limitation was the use of only 2 types of MGs. Other types of MGs could provide a different radial force or strut behavior or an alternative proximal fixation that might influence paragraft gutters and CG compression.<sup>34</sup>

Furthermore, the use of a gelatin-based water bath without flow limits the possibility of visualizing endoleaks, and no tests considering clot formation could be performed. Also, dynamic changes of the gutter sizes during the cardiac cycle, as previously shown by Overeem et al,<sup>13,35</sup> were not investigated. These issues were not aims of this study, which was a static experiment to allow accurate geometric gutter analysis.

Despite the observed size and volumes of the gutters, it remains unclear if these gutters would actually lead to clinically relevant type Ia endoleak and thereby cause sac enlargement. Presumably, the seal that was observed in the models may have been adequate to prevent type Ia endoleak.

Since preloaded deployment wires of the VSE CG could accidentally interact with the barbs of the GCE (more outstretched than GE for more hold in angled necks), it is advisable to deploy the VSE CG prior to the GCE. Balloon molding of both CGs and MGs, however, can be performed simultaneously. Alternatively, sheathed deployment could be used to prevent accidental technical problems from the wires of the VSE.

The GCE was specifically designed to treat challenging proximal necks, especially severely angulated ones. These MGs are capable of actively conforming to the proximal neck before final deployment.<sup>36</sup> Therefore it is not surprising that no differences between the 2 Excluder models were found in the current study, since our model had a straight, noncomplex landing zone. Interestingly, a significant 6-fold lower (8% vs 48%) percentage of type A1 gutters was found in setups using the GCE compared with the conventional Excluder. It seems that the proximal part of the GCE not only aligns better with angulated necks but also shortens gutters in CG setups. Future studies involving complex landing zones might provide an insight into the advantages of conformable MGs.

Because no flow model was used, spontaneous thrombosis of gutters and endoleaks could not be studied. Low flow velocity, interaction of blood with the graft, and elastic aortic wall deformation often lead to spontaneous clotting.<sup>16</sup> In addition, gutters can be treated with additional balloon dilation, EndoAnchors,<sup>20,37</sup> or liquid embolic agents.<sup>38</sup>

Compression of the CG leads to flow volume reduction, in-stent thrombosis, and potentially occlusion<sup>29,39,40</sup>; therefore, CG compression should not be underestimated. The maximum median compression was 35.9%, which can still be considered acceptable. Furthermore, compression alone is not the sole predictor of device occlusion. A landing zone in the renovisceral segment, tortuosity, and vessel diameter can all play roles.

## Conclusion

The ABX, and to a larger extent the VSE, presented lower gutter areas and gutter volumes in the current in vitro setups. The VBX showed less compression, especially compared to the ABX. Also, smaller CG/MG combinations led to smaller gutters compared to larger CG/MG combinations; however, the smaller combinations showed higher CG compression. Based on the results of this study, the authors propose use of the Conformable Excluder combined with the VSE CG, since this combination is superior to the other tested CG/MG combinations in terms of gutter size, gutter type, and CG compression. Further research is required to investigate the safest and most durable treatment options using CGs.

## Authors' Note

This study was presented at 2018 Veith Symposium (November 13–17, 2018; New York City, New York, USA); the Surgical Days (2019; Veldhoven, the Netherlands); the East Meets West meeting (September 26–28, 2019; Bucharest, Romania); and Endovascularology (October 12, 2019; Shanghai, China).

## Acknowledgments

The authors thank Gore Medical for supplying the Excluder main grafts and the Viabahn self-expanding and balloon-expandable chimney grafts. The authors thank Atrium Medical Corporation for providing the Advanta V12 stent-grafts.

## Declaration of Conflicting Interests

The author(s) declared the following potential conflicts of interest with respect to the research, authorship, and/or publication of this article: Jan D. Blankensteijn received private funding for consultancy work from W.L. Gore & Associates and Endologix. Kak K. Yeung received nonfinancial support and research grants from Atrium, Endologix, W.L. Gore & Associates, Bracco, Medac, BTG, and Cook; she received institutional grants from ICAR-AIO, ACS MD-postdoc, the VUMC fund, and the national van Walree fund.



## Funding

The author(s) received no financial support for the research, authorship, and/or publication of this article.

## ORCID iDs

Jorn P. Meekel  <https://orcid.org/0000-0002-4716-8041>

Theodorus G. van Schaik  <https://orcid.org/0000-0002-1160-1085>

Kak K. Yeung  <https://orcid.org/0000-0002-8455-286X>

## References

- Katsargyris A, Oikonomou K, Klonaris C, et al. Comparison of outcomes with open, fenestrated, and chimney graft repair of juxtarenal aneurysms: are we ready for a paradigm shift? *J Endovasc Ther.* 2013;2:159–169.
- Kirkwood ML, Chamseddin K, Arbiq GM, et al. Patient and operating room staff radiation dose during fenestrated/branched endovascular aneurysm repair using premanufactured devices. *J Vasc Surg.* 2018;5:1281–1286.
- Georgiadis GS, van Herwaarden JA, Antoniou GA, et al. Systematic review of off-the-shelf or physician-modified fenestrated and branched endografts. *J Endovasc Ther.* 2016;1:98–109.
- Ohrlander T, Sonesson B, Ivancev K, et al. The chimney graft: a technique for preserving or rescuing aortic branch vessels in stent-graft sealing zones. *J Endovasc Ther.* 2008;4:427–432.
- Coscas R, Kobeiter H, Desgranges P, et al. Technical aspects, current indications, and results of chimney grafts for juxtarenal aortic aneurysms. *J Vasc Surg.* 2011;6:1520–1527.
- Williamson AJ, Babrowski T. Current endovascular management of complex pararenal aneurysms. *J Cardiovasc Surg (Torino).* 2018;3:336–341.
- Lindblad B, Bin Jabr A, Holst J, et al. Chimney grafts in aortic stent grafting: hazardous or useful technique? Systematic review of current data. *Eur J Vasc Endovasc Surg.* 2015;6:722–731.
- Bin Jabr A, Lindblad B, Kristmundsson T, et al. Outcome of visceral chimney grafts after urgent endovascular repair of complex aortic lesions. *J Vasc Surg.* 2013;3:625–633.
- Pecoraro F, Veith FJ, Puipe G, et al. Mid- and longer-term follow up of chimney and/or periscope grafts and risk factors for failure. *Eur J Vasc Endovasc Surg.* 2016;5:664–673.
- Lachat M, Veith FJ, Pfammatter T, et al. Chimney and periscope grafts observed over 2 years after their use to revascularize 169 renovisceral branches in 77 patients with complex aortic aneurysms. *J Endovasc Ther.* 2013;20:597–605.
- Li Y, Hu Z, Bai C, et al. Fenestrated and chimney technique for juxtarenal aortic aneurysm: a systematic review and pooled data analysis. *Sci Rep.* 2016;6:20497.
- Caradu C, Berard X, Sassout G, et al. Chimney versus fenestrated endovascular aortic repair for juxta-renal aneurysms. *J Cardiovasc Surg (Torino).* 2018;4:600–610.
- Overeem SP, Donselaar EJ, Boersen JT, et al. In vitro quantification of gutter formation and chimney graft compression in chimney EVAR stent-graft configurations using electrocardiography-gated computed tomography. *J Endovasc Ther.* 2018;25:387–394.
- Donas KP, Lee JT, Lachat M, et al. Collected world experience about the performance of the snorkel/chimney endovascular technique in the treatment of complex aortic pathologies: the PERICLES registry. *Ann Surg.* 2015;3:546–553.
- Donas KP, Torsello GB, Piccoli G, et al. The PROTAGORAS study to evaluate the performance of the Endurant stent graft for patients with pararenal pathologic processes treated by the chimney/snorkel endovascular technique. *J Vasc Surg.* 2016;1:1–7.
- Moulakakis KG, Mylonas SN, Avgerinos E, et al. The chimney graft technique for preserving visceral vessels during endovascular treatment of aortic pathologies. *J Vasc Surg.* 2012;5:1497–1503.
- De Bruin JL, Yeung KK, Niepoth WW, et al. Geometric study of various chimney graft configurations in an in vitro juxtarenal aneurysm model. *J Endovasc Ther.* 2013;2:184–190.
- Yousif MY, Holdsworth DW, Poepping TL. Deriving a blood-mimicking fluid for particle image velocimetry in Sylgard-184 vascular models. In *Proceedings of the 31st Annual International Conference of the IEEE Engineering in Medicine and Biology Society: Engineering the Future of Biomedicine, EMBC 2009.* 2009;1:1412–1415.
- Mahmoodani F, Sanaei Ardekani V, See SF, et al. Optimization and physical properties of gelatin extracted from pangasius catfish (*Pangasius sutchi*) bone. *J Food Sci Technol.* 2012;11:3104–3113.
- Niepoth WW, de Bruin JL, Yeung KK, et al. A proof-of-concept in vitro study to determine if EndoAnchors can reduce gutter size in chimney graft configurations. *J Endovasc Ther.* 2013;4:498–505.
- Overeem SP, Boersen JT, Schuurmann RCL, et al. Classification of gutter type in parallel stenting during endovascular aortic aneurysm repair. *J Vasc Surg.* 2017;2:594–599.
- Koo TK, Li MY. A guideline of selecting and reporting intraclass correlation coefficients for reliability research. *J Chiropr Med.* 2016;2:155–163.
- Ronchey S, Fazzini S, Scali S, et al. Collected transatlantic experience from the PERICLES registry: use of chimney grafts to treat post-EVAR type Ia endoleaks shows good midterm results. *J Endovasc Ther.* 2018;4:492–498.
- Starnes BW. Physician-modified endovascular grafts for the treatment of elective, symptomatic, or ruptured juxtarenal aortic aneurysms. *J Vasc Surg.* 2012;3:601–607.
- Starnes BW, Heneghan RE, Tatum B. Midterm results from a physician-sponsored investigational device exemption clinical trial evaluating physician-modified endovascular grafts for the treatment of juxtarenal aortic aneurysms. *J Vasc Surg.* 2017;2:294–302.
- Glorion M, Coscas R, McWilliams RG, et al. A comprehensive review of in situ fenestration of aortic endografts. *Eur J Vasc Endovasc Surg.* 2016;6:787–800.
- Le Houérou T, Fabre D, Alonso CG, et al. In situ antegrade laser fenestrations during endovascular aortic repair. *Eur J Vasc Endovasc.* 2018;3:356–362.
- Mendes BC, Oderich GS. Selection of optimal bridging stents for fenestrations and branches. In: Oderich GS, ed. *Endovascular Aortic Repair: Current Techniques with*

- Fenestrated, Branched and Parallel Stent-Grafts*. Heidelberg, Germany: Springer; 2017:359–374.
29. Mestres G, Uribe JP, García-Madrid C, et al. The best conditions for parallel stenting during EVAR: An in vitro study. *Eur J Vasc Endovasc Surg*. 2012;5:468–473.
  30. Boersen JT, Donselaar EJ, Groot Jebbink E, et al. Benchtop quantification of gutter formation and compression of chimney stent grafts in relation to renal flow in chimney endovascular aneurysm repair and endovascular aneurysm sealing configurations. *J Vasc Surg*. 2017;5:1565–1573.
  31. Barnes RW. Hemodynamics for the vascular surgeon. *Arch Surg*. 1980;2:216–223.
  32. Sutura SP, Skalak R. The history of Poiseuille's law. *Annu Rev Fluid Mech*. 1993;25:1–20.
  33. Yamine H, Briggs CS, Stanley GAA, et al. Advanced techniques for treating juxtarenal and pararenal abdominal aortic aneurysms: chimneys, periscopes, sandwiches and other methods. *Tech Vasc Interv Radiol*. 2018;3:165–174.
  34. De Bock S, Iannaccone F, De Beule M, et al. Filling the void: a coalescent numerical and experimental technique to determine aortic stent graft mechanics. *J Biomech*. 2013;14:2477–2482.
  35. Overeem SP, de Vries JPM, Boersen JT, et al. Haemodynamics in different flow lumen configurations of customised aortic repair for infrarenal aortic aneurysms. *Eur J Vasc Endovasc Surg*. 2019;5:709–718.
  36. Rhee R, Peterson B, Moore E, et al. Initial human experience with the GORE EXCLUDER Conformable AAA endoprosthesis. *J Vasc Surg Cases Innov Tech*. 2019;5:319–322.
  37. Donselaar EJ, Van Der Vijver-Coppen RJ, Van Den Ham LH, et al. EndoAnchors to resolve persistent type Ia endoleak secondary to proximal cuff with parallel graft placement. *J Endovasc Ther*. 2016;23:225–228.
  38. Henrikson O, Roos H, Falkenberg M. Ethylene vinyl alcohol copolymer (Onyx) to seal type 1 endoleak. A new technique. *Vascular*. 2011;2:77–81.
  39. Rancic Z, Pfammatter T, Lachat M, et al. Periscope graft to extend distal landing zone in ruptured thoracoabdominal aneurysms with short distal necks. *J Vasc Surg*. 2010;5:1293–1296.
  40. Scali ST, Feezor RJ, Huber TS. Acute bilateral renal artery chimney stent thrombosis after endovascular repair of a juxtarenal abdominal aortic aneurysm. *J Vasc Surg*. 2015;4:1058–1061.